

Adaptive multiresolution for the simulation of multi-species, compressible, viscous flows.

Christian TENAUD ¹

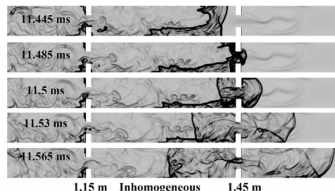
¹Laboratoire EM2C - CNRS UPR 288, Gif-Sur-Yvette, France.

Evian-Le-Bains; 14th June 2022



Introduction

Multiple time and space scales: flame acceleration in H_2 / Air mixing.



From L. R. Boeck *et al.* (2016), *Shock Waves* 26: 181–192.

Simulations need **capturing time and space multiple scales**
from 1 m à 100 μ m and from 1 s à 10 μ s

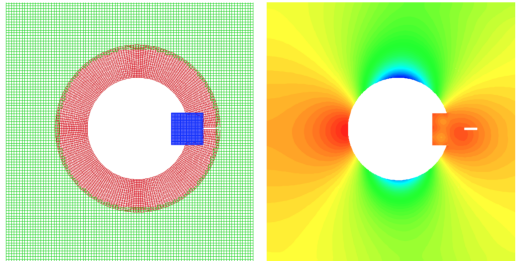
- Compressible effects: high gradients and discontinuities;
- Thermodiffusive instabilities and turbulence;
- Large Temperature variation, localised chemical reactions;
- Flame acceleration and transition to detonation structures.

High-order approximations coupled with dynamic grid adaption.

Multi-level techniques.

- Multi-level adaptive technique (MLAT) [Brandt (1977)]:
Adaptive discretization and Multi-Grid methods
- Method of assembling overlapping grids - Chimera method
[Volkov (1968), Steger *et al.* (1983), Peron & Benoît (2013)]

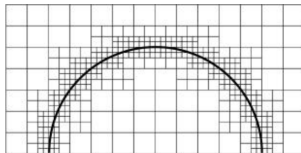
- Manage overlapping with ghost cells
- Well adapted for complex geometries (local geometrical details)
- Well adapted for sliding mesh



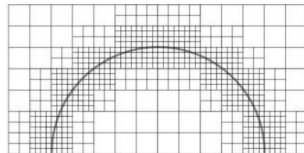
From Peron, PhD Thesis (2014).

Adaptive grid techniques.

- AMR [Berger, Oliger, Collela (1984–1989)]:
 - ▷ Cell- / Block-, and Patch-based AMR: [Dunning *et al.* (2020), Gunney *et al.* (2006–2017), Berger *et al.* (1984–1998)]

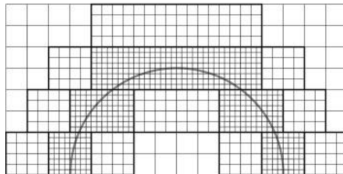


Cell-based AMR with 382 cells

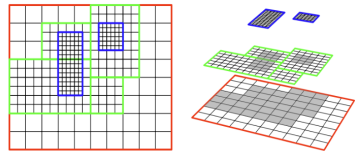


Block-based AMR with 596 cells

From Dunning *et al.* (2020)



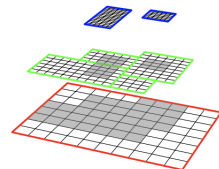
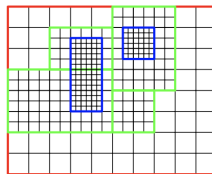
Patch-based AMR with 836 cells



From Gunney *et al.* (2013)

Adaptive grid techniques.

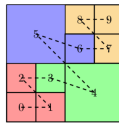
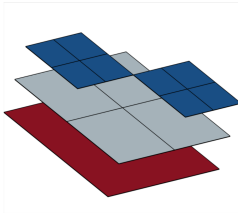
- ▷ Block-, and Patch-based AMR: [Berger *et al.* (1984–1998), Gunney *et al.* (2006–2017)]
 - Advantage of regular grid;
 - But refines large sub-sections;
 - Manage boundary conditions / ghost cells;
 - Manage Proxy / Mapping connectors;
 - Allows divisions ≥ 2 ;
- Several softwares: SAMRAI, AMRClaw, AMROC, AMReX, PARAMESH, BoxLib, SAMURAI, ...



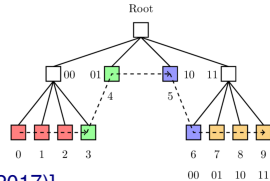
From [Gunney *et al.* (2013)]

Adaptive grid techniques.

- ▶ Cell-based AMR: [De Zeeuw & Powell (1993), Khokhlov (1998), Dunning *et al.* (2020)]
 - Generally based on binary trees (octree);
 - Limit cell number near gradient;
 - Manage boundary conditions / ghost cells;
 - Several softwares: [P4est](#), [PABLO](#), [CLAMR](#), [SAGE/RAGE](#), [SAMURAI](#), ...

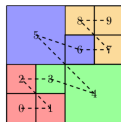
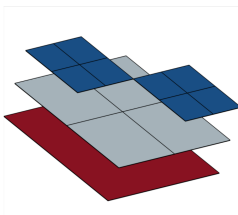


From [Drui *et al.* (2017)]

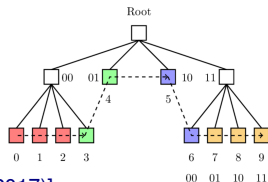


Adaptive grid techniques.

- ▷ Cell-based AMR: [De Zeeuw & Powell (1993), Khokhlov (1998), Dunning *et al.* (2020)]
 - Generally based on binary trees (octree);
 - Limit cell number near gradient;
 - Manage boundary conditions / ghost cells;
 - Several softwares: [P4est](#), [PABLO](#), [CLAMR](#), [SAGE/RAGE](#), [SAMURAI](#), ...



From [Drui *et al.* (2017)]



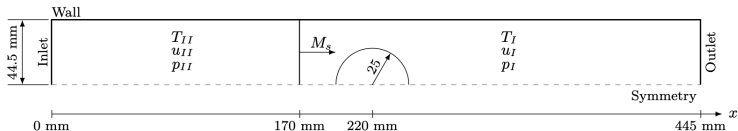
- based on ad hoc heuristic criteria ;
 - difficult to control refinement error $\|Q^{(AMR)} - Q^{(UGF)}\|$
- ⇒ Adjoint-based error estimate for AMR [Narechania *et al.* (2017)]: mainly for steady or slowly evolving flows. [Cart3D](#).

Multiresolution techniques.

● MRA : Multi-Resolution Analysis

- ▷ Harten (1994-1995): multirésolution & syst. hyperbolique;
- ▷ Cohen *et al.* (2003): formalisme base d'ondelettes, multirésolution complètement adaptative;
- ▷ Brix *et al.* (2011): Data structures, implementation and parallelization;
- ▷ Duarte *et al.* (2013): MRA coupled with time adaptive method;
- ▷ Deiterding *et al.* (2020): MRA into AMROC, comparisons.

Shock wave ($M_s = 1.22$) interacting with R_{22} bubble [Haas & Sturtevant (1987)]





Nested grids

Dyadic grids: Grid level : $l \in [0, L]$
Cell referenced by position and
grid-level: (j, l)

$$(j, l) \rightarrow (2j, l+1), (2j+1, l+1)$$

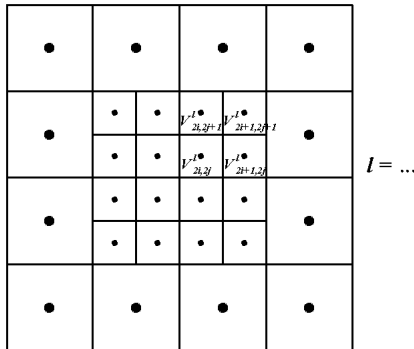
$$\Omega = \bigcup_{j \in I_l} V_j^l \text{ with } |V_j^l \cap V_k^l| = 0,$$

for $j \neq k; j, k \in I_l$.

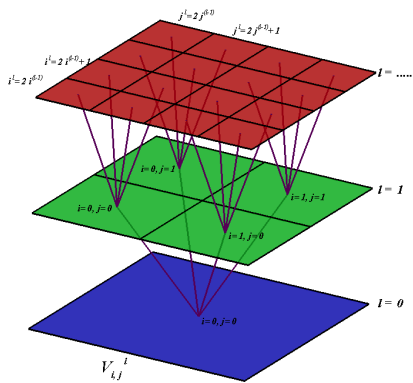
Refinement process:

$$V_j^l = \bigcup_{p \in \mathcal{C}_j^l} V_p^{l+1},$$

\mathcal{C}_j^l set of *children* indexes of V_j^l .



Tree data Structure



•	•	$V_{2i, 2j+1}^2$	$V_{2i+1, 2j+1}^2$	$l = 2$
•	•	$V_{2i, 2j}^2$	$V_{2i+1, 2j}^2$	
$V_{0,1}^2$	$V_{1,1}^2$	•	•	
$V_{0,0}^2$	$V_{1,0}^2$	•	•	

Terminology: *father* $(j/2, l-1)$; *children* $(2j, l+1), (2j+1, l+1)$; *cousin* $(j+1, l), (j-1, l)$
leaves are upper elements (with no *child*)



Projection operator:

$\mathbf{P}_{l+1 \rightarrow l}$: compute \mathbf{v}_j^l knowing *children*-cells $\mathbf{v}_{2j}^{l+1}, \mathbf{v}_{2j+1}^{l+1}, \dots$

Nested grid: operator is *exact* and *unique* [A. Cohen *et al.* (2000)]:

Assuming cell average as: $(\mathbf{v}_j^l)^n = \frac{1}{|V_j^l|} \int_{V_j^l} \mathbf{w}(\mathbf{x}, n \delta t) d\mathbf{x}$

Projection operator:

$$\mathbf{P}_{l+1 \rightarrow l} : \mathbf{v}_j^l = \frac{1}{|V_j^l|} \sum_{p \in \mathcal{C}_j^l} |V_p^{l+1}| \mathbf{v}_p^{l+1};$$

\mathcal{C}_j^l index set of the $2^{N_{dim}}$ *children*-cells at grid-level $l + 1$, for current cell V_j^l .

Prediction operator:

$\mathbf{P}_{l \rightarrow l+1}$: maps \mathbf{v}^l to an approximate value $\hat{\mathbf{v}}^{l+1}$ of \mathbf{v}^{l+1} .

$\mathbf{P}_{l \rightarrow l+1}$ is not unique and **prediction** needs to be:

- *local*; interpolation stencil must contain the *parent*-cell and its nearest neighbors in each direction [A. Cohen *et al.* (2000), M. Postel (2001)].
- *consistent with the projection operator*, i.e. $\mathbf{P}_{l+1 \rightarrow l} \circ \mathbf{P}_{l \rightarrow l+1} = Id$.

Conservativity:

$$|V_j^l| v_j^l = \sum_{p \in \mathcal{C}_j^l} |V_p^{l+1}| \hat{v}_p^{l+1}$$

- *linear* (not mandatory...) \rightarrow simplicity of the numerical analysis.
Information on non-linear operator found in [F. Anrandiga *et al.* (1999)]

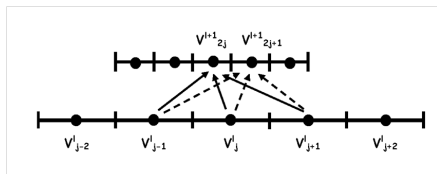
Prediction operator: interpolation

Prediction interpolation: centered linear polynomial

$$\mathbf{P}_{l \rightarrow l+1} : \begin{cases} \hat{v}_{2j}^{l+1} = v_j^l + \sum_{q=1}^s \xi_q (v_{j+q}^l - v_{j-q}^l), \\ \hat{v}_{2j+1}^{l+1} = v_j^l - \sum_{q=1}^s \xi_q (v_{j+q}^l - v_{j-q}^l), \end{cases}$$

Coefficients of centered linear polynomial:

order (o)	s	ξ_1	ξ_2
1	0	0	0
3	1	$-\frac{1}{8}$	0
5	2	$-\frac{22}{128}$	$\frac{3}{128}$



for $s = 1$



Prediction operator: multi-D interpolations

Extension to multidimensional Cartesian grids:

Tensorial product of 1-D operator [B.L. Bihari & A. Harten (1997), O. Roussel *et al.* (2003)].

2D-interpolation

$$\hat{v}_{2j+p, 2k+q}^{l+1} = v_{j,k}^l + (-1)^p Q^s(j; \mathbf{v}'_{\cdot, k}) + (-1)^q Q^s(k; \mathbf{v}'_{j, \cdot}) - (-1)^{(p+q)} Q_2^s(j, k; \mathbf{v}^l),$$

with $p, q \in [0, 1]$ and:

$$Q^s(j; \mathbf{v}^l) = \sum_{q=1}^s \xi_q \left(v_{j+q}^l - v_{j-q}^l \right),$$

$$Q_2^s(j, k; \mathbf{v}^l) = \sum_{a=1}^s \xi_a \sum_{b=1}^s \xi_b \left(v_{j+a, k+b}^l - v_{j-a, k+b}^l - v_{j-a, k-b}^l + v_{j+a, k-b}^l \right).$$



Prediction operator: *details*

prediction error: *details* (d_j^l)

details

$$\mathbf{d}_j^l = \mathbf{v}_j^l - \hat{\mathbf{v}}_j^l.$$

Consistency assumption [A. Harten (1995)]: $\sum_{p \in C_j^l} |V_p^l| d_p^l = 0$.

Knowing $2^{N_{dim}}$ cell-averages $\mathbf{v}_j^{l+1} \Leftrightarrow$ knowing \mathbf{v}_j^l and $(2^{N_{dim}} - 1) \mathbf{d}_j^l$:

$$\mathbf{v}_{2k}^{l+1} = \hat{\mathbf{v}}_{2k}^{l+1} + \mathbf{d}_{2k}^{l+1};$$

$$\mathbf{v}_{2k+1}^{l+1} = \frac{|V_j^l|}{|V_{2k+1}^{l+1}|} \mathbf{v}_j^l - \mathbf{v}_{2k}^{l+1}.$$



Prediction operator: *details*

Polynomial accuracy

$$|\mathbf{d}^l| \leq C 2^{-l} |\mathbf{v}^l|_{L^\infty(V_j^l)}.$$

Main property for MR process:

- Solution with locally bounded σ -th order derivatives [A. Cohen *et al.* (1992)];

$$|\mathbf{d}^l| = 0.$$

- Decay with 2^{-l} for solutions smooth enough;
- Significantly high *detail* values within singularities.

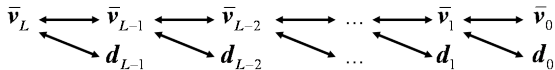
Multiresolution transform:

$$\mathbf{D}^l = \left\{ d_j^l, 0 \leq j \leq N_l \right\}, \quad \text{with } N_l = (2^{N_{dim}} - 1) 2^{N_{dim}(l-1)}$$

$$\mathbf{v}^{(l+1)} \mapsto \left(\mathbf{v}^l, \mathbf{D}^{l+1} \right).$$

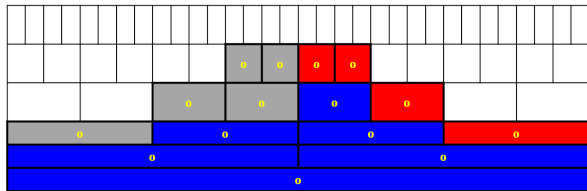
One to one transformation: from *leaves* down to the root

$$\mathcal{M} : \mathbf{v}^L \mapsto \left(\mathbf{v}^0, \mathbf{D}^1, \dots, \mathbf{D}^L \right) = \mathbf{M}^L.$$



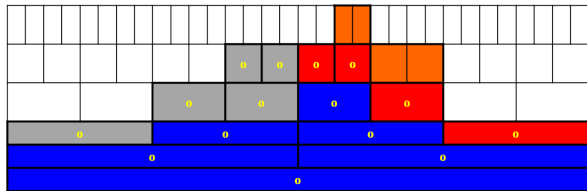
Thresholding and Tree pruning/enlargement, graded Tree:

- Thresholding: $|\mathbf{d}'|_{L_1} < \varepsilon_I \Rightarrow \text{cell discarded};$



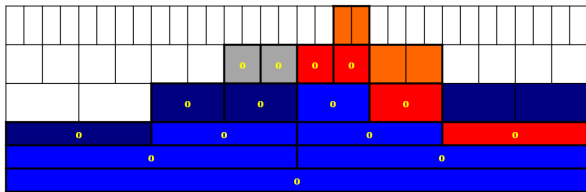
Thresholding and Tree pruning/enlargement, graded Tree:

- Thresholding: $|\mathbf{d}'|_{L_1} < \varepsilon_I \Rightarrow$ cell discarded;
- Enlarge the tree for foreseeing discontinuity: $|\mathbf{d}'|_{L_1} \geq \varepsilon_I$ and $|\mathbf{d}'|_{L_1} \geq 2^p \varepsilon_I$



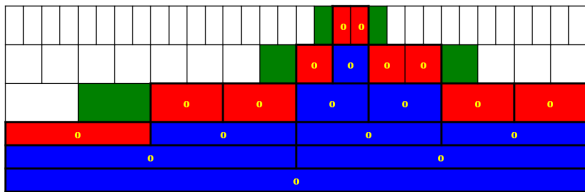
Thresholding and Tree pruning/enlargement, graded Tree:

- Thresholding: $\left| \mathbf{d}' \right|_{L_1} < \varepsilon_l \Rightarrow$ cell discarded;
- Enlarge the tree for foreseeing discontinuity: $\left| \mathbf{d}' \right|_{L_1} \geq \varepsilon_l$ and $\left| \mathbf{d}' \right|_{L_1} \geq 2^p \varepsilon_l$
- Building graded tree:
if $(j, l) \in \tilde{\Lambda}_{\varepsilon_l}$ then $(j/2 + q, l-1) \in \tilde{\Lambda}_{\varepsilon_l}$; $q \in [-s, +s]$



Thresholding and Tree pruning/enlargement, graded Tree:

- Thresholding: $\left| \mathbf{d}' \right|_{L_1} < \varepsilon_l \Rightarrow$ cell discarded;
- Enlarge the tree for foreseeing discontinuity: $\left| \mathbf{d}' \right|_{L_1} \geq \varepsilon_l$ and $\left| \mathbf{d}' \right|_{L_1} \geq 2^p \varepsilon_l$
- Building graded tree:
if $(j, l) \in \tilde{\Lambda}_{\varepsilon_l}$ then $(j/2 + q, l - 1) \in \tilde{\Lambda}_{\varepsilon_l}$; $q \in [-s, +s]$
- Add virtual *leaves* for flux conservation



Thresholding: control

Approximation MR operator: $\mathcal{A}_{\Lambda_{\varepsilon_l}}$

$$\|\mathbf{v}^L - \mathcal{A}_{\Lambda_{\varepsilon_l}} \mathbf{v}^L\| = C \sum_{|\mathbf{d}^l| < \varepsilon_l} |\mathbf{d}^l| 2^{-N_{dim} l}$$

Control of the thresholding effect **Harten (1994)**:

$$\varepsilon_l = 2^{N_{dim} \cdot (l-L)} \varepsilon$$

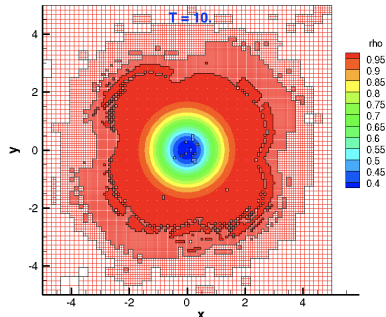
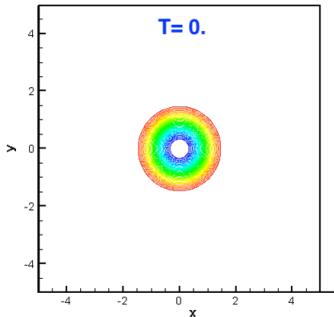
Knowing ε : $\|\mathbf{v}^L - \mathcal{A}_{\Lambda_{\varepsilon_l}} \mathbf{v}^L\| \leq C\varepsilon$

2D Vortex advection: solution

Strong vortex propagated at 45° by a supersonic flow:

$$(\delta u, \delta v) = \frac{\varepsilon}{2\pi} e^{0.5(1-r^2)} (-y, x) ; \quad \delta T = -\frac{(\gamma - 1)\varepsilon^2}{8\pi^2} e^{0.5(1-r^2)} ; \quad \delta S = 0.$$

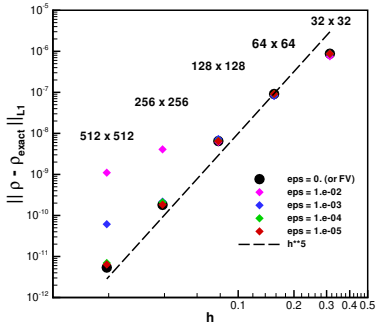
$$\varepsilon = 5; \quad (\rho, u, v, P) = (1, 1, 1, 1) \quad \text{and} \quad (x \times y) = [-5, 5] \times [-5, 5]$$



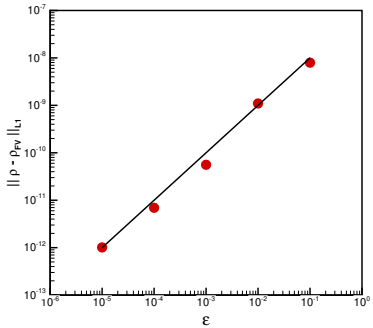


Euler 2D Vortex advection: Error analysis

Error / Exact solution

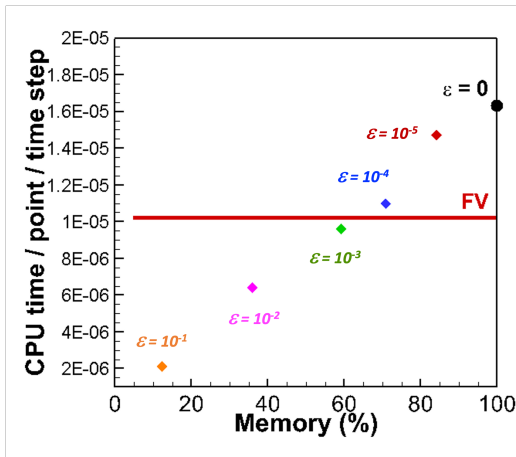


Perturbation Error $T = 10$



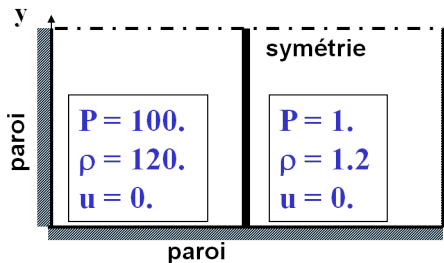
Euler 2D Vortex advection: Efficiency

- $\text{CPU}(\varepsilon = 0) = 2. \times \text{CPU}(\text{FV})$
- Memory Compression: $\forall \varepsilon$
 - $\varepsilon > 10^{-3}$: 60 % (FV)
 - $\varepsilon > 10^{-2}$: 35 % (FV)
- $\varepsilon > 10^{-3} \Rightarrow \text{CPU Gains if 50 \% FV-Mem saved}$

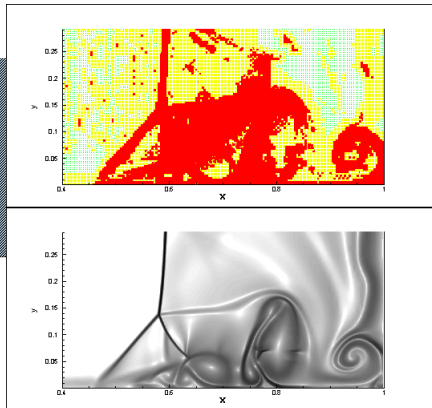


2D Viscous shock tube: MR 9 grid levels, $\varepsilon = 10^{-2}$, $s = 1$

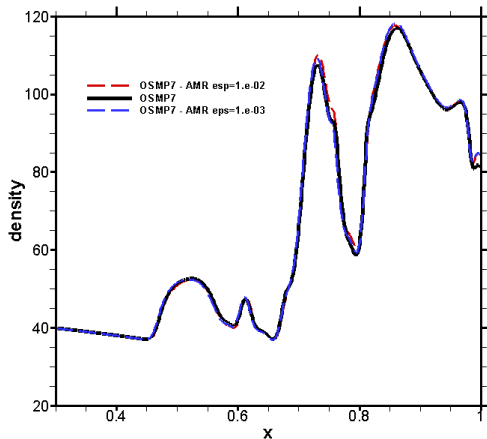
$$T = 1.$$



$$L_x = 1 ; L_y = 0.5$$



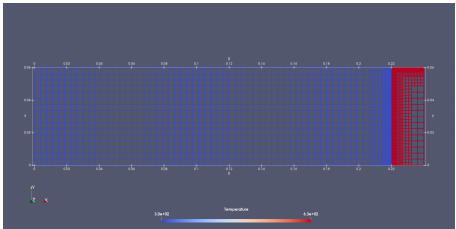
$\varepsilon = 10^{-2} \Rightarrow$ **Memory compression = 70 %; CPU ratio: $t^{MR} / t^{FV} = 20 \%$**

2D Viscous shock tube: video MR 9 grid levels, $\varepsilon = 10^{-2}$, $s = 1$ MR - 9 grid levels: (1024×512) - Reference: FV-OSMP7 (1000×5000) 

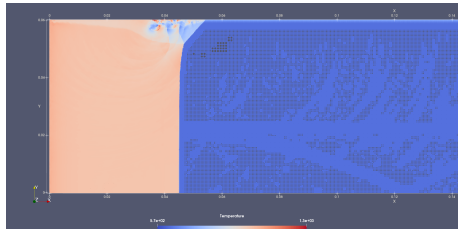


Tube: MR 8 levels (16×4 trees $\equiv 4096 \times 1024$), $\varepsilon = 10^{-3}$, $s = 1$

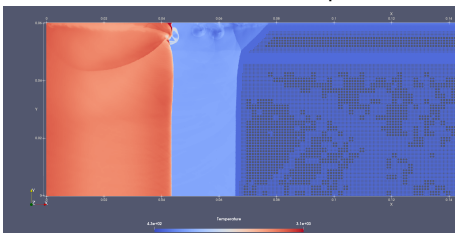
$t = 0$ s; 99.5 % compression



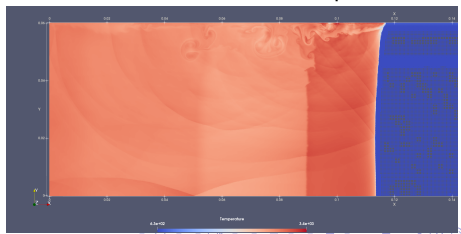
$t = 40 \times 10^{-5}$ s; 80 % compression



$t = 45 \times 10^{-5}$ s; 78 % compression



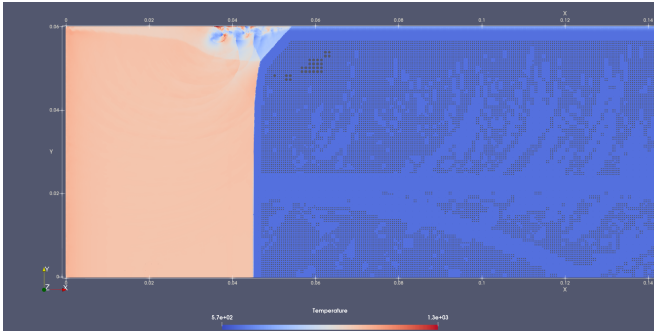
$t = 50. \times 10^{-5}$ s; 77 % compression





Tube: MR 8 levels (16×4 trees $\equiv 4096 \times 1024$), $\varepsilon = 10^{-3}$, $s = 1$

OpenMP: 32 cores - parallelization delicate for grid adaption.





● **Multiresolution technique:**

- Assess capability of the adaptive multiresolution technique for compressible viscous flows;
- Accuracy controlled by the perturbation error: threshold parameter ($\varepsilon \lesssim 10^{-3}$)
- Must be coupled with high-order numerical scheme;
- Attractive approach because of a priori error control;
- Powerful but hard to handle: Speed up if Mem. < 50 %;

● **Work in progress:**

- Coupled with Immersed Boundary conditions;
- Emphasize on parallel algorithm:
 - Reflect on an efficient data organization;
 - Hard task for effective load balancing;
 - See [SAMURAI software](#).